DOI: https://doi.org/10.15276/aait.07.2024.20
UDC 681.5.015.52

Evaluation of the accuracy of human eye movement system identification using step test signals

Vitaliy D. Pavlenko[1)]
ORCID: https://orcid.org/0000-0002-5655-4171; pavlenko_vitalij@ukr.net. Scopus Author ID: 54401442600
Denys K. Lukashuk[1)]
ORCID: https://orcid.org/0009-0003-3149-3741; user111228322@gmail.com
[1)] Odesa Polytechnic National University, 1, Shevchenko Ave. Odesa, 65044, Ukraine

ABSTRACT

This study investigates nonlinear dynamic system identification methods to simulate the human eye movement system (EMS), focusing on the accurate representation of transient characteristics derived from step test signals. Integral nonlinear models were applied to capture the nonlinear dynamics and inertial properties of the EMS. Experimental "input-output" data were collected using advanced eye-tracking technology, enabling the identification of multidimensional transient characteristics (MTCs) that describe the EMS's dynamic behavior in response to visual stimuli. The research utilized approximation and compensation methods to develop models based on integro-power series (IPS), while the least squares method (LSM) was applied to construct integro-power polynomial (IPP) models. The compensation method, while less computationally demanding, showed lower accuracy, making it less applicable for tasks requiring high precision. Third-order models exhibited instability in their transient characteristics, limiting their practical use. Second-order models, specifically quadratic IPP models developed with LSM, proved to be the most accurate and computationally efficient. These models provided precise and consistent representations of EMS dynamics, with error rates significantly reduced when using three test signal responses instead of two. This emphasizes the importance of sufficient data in improving model reliability. The findings highlight the suitability of the quadratic IPP model refined with LSM for further investigations. This model offers a robust basis for advancing research into personalized psychophysiological condition assessment through the development of classifiers. Its accuracy and stability make it a valuable tool for exploring state classification methodologies in healthcare, cognitive science, and related domains requiring precise dynamic system simulation.

Keywords: Eye movement system; simulation; Volterra models; eye-tracking technology; accuracy of simulation; neurophysiological condition

***For citation*: Pavlenko V. D., Lukashuk D.K. "Evaluation of the accuracy of human eye movement system identification using step test signals". *Applied Aspects of Information Technology.* 2024; Vol. 7 No. 4: 301–312. DOI: https://doi.org/10.15276/aait.07.2024.20**

1. INTRODUCTION

Eye-tracking technology has emerged as a powerful tool for evaluating neurocognitive health, particularly in conditions like Alzheimer's [1], [2], [3] and Parkinson's [4] diseases. Studies indicate that eye-tracking data, by detecting characteristic ocular movement patterns, can aid in the early diagnosis of these conditions, offering a non-invasive approach for health monitoring. Eye-tracking has also been applied in posttraumatic stress disorder (PTSD) research, where it helps identify attentional biases toward negative stimuli, contributing to better understanding and potential early diagnosis of the disorder [5]. Furthermore, recent research suggests that eye-tracking can serve as an effective tool for autism diagnosis, with particular biomarkers in eye movements being indicative of autism spectrum disorder [6].

Additionally, eye-tracking technology has shown considerable potential in dyslexia research. By examining specific eye movement patterns in dyslexic individuals, researchers have identified characteristic behaviors that inform targeted interventions. This has paved the way for creating customized educational solutions, aimed at improving reading outcomes and cognitive engagement for dyslexic readers [7], [8].

Eye-tracking is not limited to medical applications; it has gained traction in the fields of education and social sciences. In online learning environments [9], eye movement data can reveal attention patterns and cognitive engagement, allowing for tailored learning interventions that optimize student engagement and minimize cognitive load. Expanding the application of eye-tracking to professional environments has provided insights that improve the efficiency of various work processes [10], [11] and support teamwork in training sessions, especially in complex healthcare environments [12]. Moreover, eye-tracking data holds promise for enhancing security by enabling gaze-based authentication methods for data access control [13], [14].

Research on the application of eye-tracking technology also extends to anomaly detection, where parametric and nonparametric analyses help identify irregular patterns that could indicate cognitive or neurological issues. For instance, detecting anomalies in eye movement can be used in assessments related to mental workload and multitasking capabilities [15], [16]. Such methodologies are not only relevant in healthcare but can also contribute to safety assessments in high-risk industries, supporting the early detection of cognitive strain among workers, particularly in fields requiring high mental acuity [17, 18], [19]. Further developments in eye-tracking have been explored in ocular disease diagnostics through deep learning techniques, where transfer learning models significantly improve classification accuracy for early eye disease detection [20], [21].

This study focuses on simulating the human eye movement system (EMS) using Volterra models, enabling the evaluation of model precision and computational efficiency. By applying nonlinear modeling techniques, we aim to establish a framework that accurately represents human ocular dynamics. This approach allows for determining the most accurate and computationally efficient model, with practical implications for its effectiveness in applications.

2. PROBLEM STATEMENT

To simulate the human eye movement system, integral nonlinear models [22, 23], [24, 25], [26] are employed, which consider both the nonlinear and inertial properties of the system being studied. The EMS is simulated by determining multidimensional transient characteristics (MTCs) based on "input-output" experimental data [25]. Eye-tracking technology is used to collect these experimental data, enabling accurate recording of eye responses to visual stimuli. The construction of the model involves an approximation simulation method using integro-power series (IPS) [26], [27], [28] and a least squares method (LSM) [26], [29, 30], [31] to create the model based on integro-power polynomials (IPP). The simulation methods for nonlinear dynamic systems (NDS) based on IPS and IPP vary in their computational approaches, providing distinct methodologies for NDS simulation [28].

The objective of this research is to rigorously evaluate EMS simulation accuracy, selecting the most precise and computationally efficient nonlinear dynamic model based on IPS and IPP methods. The optimal model will then be used to construct feature spaces tailored to individual psychophysiological profiles, enhancing reliability in assessing personalized conditions. This study also addresses the development of algorithmic and software tools for extracting EMS dynamic characteristics from eye-tracking data and systematically comparing the effectiveness of different simulation methods.

3. THEORETICAL BACKGROUND

In this study, the approximation method [28] and compensation method [26] are employed to develop models using IPS, while the least squares method (LSM) [24] is utilized for constructing models based on IPP.

Approximation Identification Method. The approximation identification method for NDS (method of linear combinations of responses) in the time domain is grounded in isolating the *n*-th partial component (PC) of the NDS response by constructing linear combinations of responses to test signals with different amplitudes. This approach is an adaptation of methods originally based on the Volterra series. It is proved in [26] that:

Assertion 1. Let test signals $a_1x(t)$, $a_2x(t),\ldots,a_Nx(t)$ be sequentially applied to the input of the NDS, where N is the degree; $a_1, a_2,\ldots,a_N$ are different real numbers, non-zero, satisfying the condition $|a_j| \le 1$ for $\forall j=1,2,...,N$; $x(t)$ is an arbitrary function. Then, the linear combination of the system's responses to these inputs equals the n-th PC of the response to the input signal $x(t)$ with an accuracy up to the discarded terms Δ of the IPS of order $N+1$ and higher:

$$\sum_{j=1}^{N} c_j y[a_j x(t)] = y_n[x(t)] + \Delta, \qquad (1)$$

where

$$y_n[x(t)] = y_n(t),$$

$$y[a_j x(t)] = \sum_{n=1}^{\infty} a_j^n \int_0^t \ldots \int_0^t w_n(t-\tau_1,...,t-\tau_n) \prod_{i=1}^{n} x(\tau_i) d\tau_i;$$

$$\Delta = \sum_{j=1}^{N} c_j \sum_{n=N+1}^{\infty} y_n[x(t)],$$

if c_j are real coefficients such that

$$\mathrm{A}_N \, \mathrm{c} = \mathrm{b}, \qquad (2)$$

where

$$\mathrm{A}_N = \begin{bmatrix} a_1 & a_2 & \ldots & a_N \\ a_1^2 & a_2^2 & \ldots & a_N^2 \\ \ldots & \ldots & \ldots & \ldots \\ a_1^N & a_2^N & \ldots & a_N^N \end{bmatrix}, \quad \mathrm{c} = \begin{bmatrix} c_1 \\ c_2 \\ \ldots \\ c_N \end{bmatrix}, \quad \mathrm{b} = \begin{bmatrix} b_1 \\ b_2 \\ \ldots \\ b_N \end{bmatrix},$$

here $b_l = 1$ when $l = n$; $b_l = 0$ when $l \neq n$, $\forall l \in \{1,2,\ldots,N\}$.

The system (2) always has a solution, and it is unique since its determinant differs from the Vandermonde determinant only by the factor a_1, $a_2,\ldots,a_N$. Thus, for any real numbers a_j, which are non-zero and pairwise distinct, it is possible to find numbers c_j such that the linear combination (1) of the NDS responses equals the n-th term of the IPS with an accuracy up to the discarded terms of the series. By satisfying the conditions for forming the system of linear algebraic equations (2), we obtain the relation (1).

When test signals in the form of step functions (Heaviside functions – $\theta(t)$) with amplitudes a_1, $a_2,\ldots,a_N$ are applied to the input of the system being identified, we obtain estimates of the diagonal cross-sections of the NDS multidimensional transient characteristics:

$$\hat{h}_n(t,\ldots,t) = \hat{y}_n(t) = \sum_{j=1}^{N} c_j^{(n)} y(a_j\theta(t)) = c_1^{(n)} y(t \mid a_1) + \\ + c_2^{(n)} y(t \mid a_2) + \ldots + c_N^{(n)} y(t \mid a_N) + \Delta_n, n = \overline{1,N}; \quad (3)$$

where $y(t \mid a_j) = y(a_j\theta(t))$ are the NDS responses to the test signal with amplitude a_j, and Δ_n represents the methodological error resulting from the discarded terms of the IPS of order $n+1$ and higher.

Fig. 1 shows a structural scheme demonstrating the calculation of the diagonal cross-section of the second-order transient characteristic based on three test signals. This scheme is a particular application of formulas (2) and (3), illustrating how the step test signals are processed through the NDS to yield the transient characteristic.

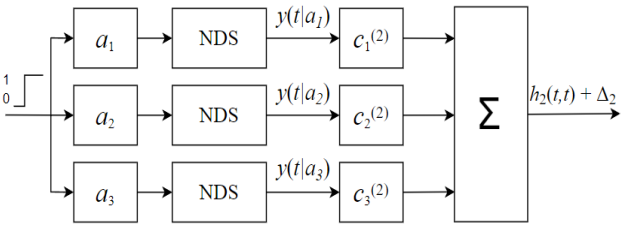

Fig. 1. **Structural scheme for computing the diagonal cross-section of the second-order transient characteristic using the approximation identification method**

Source: **compiled by the authors**

Identification of NDS using the Least Squares Method. The method of NDS identification based on the Volterra polynomial model in the time domain relies on approximating the NDS response $y(t)$ to an arbitrary deterministic signal $x(t)$ in the form of an IPP of N-th order (N – the order of the approximation model):

$$y_N(t) = \sum_{n=1}^{N} \hat{y}_n(t) = \\ = \sum_{n=1}^{N} \int_0^t \ldots \int_0^t w_n(t-\tau_1,\ldots,t-\tau_n) \prod_{i=1}^{n} x(\tau_i) d\tau_i. \quad (4)$$

Valid assertion [26].

Assertion 2. Let test signals $a_1x(t)$, $a_2x(t)$, …, $a_Lx(t)$ be sequentially applied to the input of the NDS; a_1, $a_2,\ldots,a_L$ are different real numbers satisfying the condition $0<|a_j|\leq 1$ for $\forall j=1,2,\ldots,L$; $x(t)$ is an arbitrary deterministic signal, then

$$\tilde{y}_N(a_j x(t)) = \sum_{n=1}^{N} \hat{y}_n(a_j x(t)) = \\ = \sum_{n=1}^{N} a_j^n \int_0^t \ldots \int_0^t w_n(t-\tau_1,\ldots,t-\tau_n) \prod_{i=1}^{n} x(\tau_i) d\tau_i = \quad (5) \\ = \sum_{n=1}^{N} a_j^n \hat{y}_n(t) \text{ for } \forall j,\ j = \overline{1,L}, L \geq N.$$

The partial components in the approximation model $\hat{y}_n(t)$ are found using the least squares method. This allows obtaining estimates for them, where the sum of squares of deviations of the NDS responses being identified, $y[a_j x(t)]$ from the model responses $\tilde{y}_N[a_j x(t)]$, is minimal, thus ensuring the minimum mean square criterion

$$J_N = \sum_{j=1}^{L} \left(y(a_j x(t)) - \tilde{y}_N(a_j x(t))\right)^2 = \\ = \sum_{j=1}^{L} \left(y(t \mid a_j) - \sum_{n=1}^{N} a_j^n \hat{y}_n(t) \right)^2 \to \min. \quad (6)$$

Minimizing criterion (6) boils down to solving a system of normal equations Gauss, which in vector-matrix form can be expressed as:

$$\mathrm{A}'\mathrm{A}\hat{\mathrm{y}} = \mathrm{A}'\,\mathrm{y}, \quad (7)$$

where

$$\mathrm{A} = \begin{bmatrix} a_1 & a_1^2 & \cdots & a_1^N \\ a_2 & a_2^2 & \cdots & a_2^N \\ \cdots & \cdots & \cdots & \cdots \\ a_L & a_L^2 & \cdots & a_L^N \end{bmatrix}, \quad \mathrm{y} = \begin{bmatrix} y(t \mid a_1) \\ y(t \mid a_2) \\ \cdots \\ y(t \mid a_L) \end{bmatrix}, \quad \hat{\mathrm{y}} = \begin{bmatrix} \hat{y}_1(t) \\ \hat{y}_2(t) \\ \cdots \\ \hat{y}_N(t) \end{bmatrix}.$$

If the identified system is supplied with test signals in the form of step functions with amplitudes a_1, $a_2,\ldots,a_L$, we obtain estimates of the transient characteristics $\hat{h}_1^{(N)}(t)$ and the diagonal cross-

sections of the transient characteristics of the eye movement system $\hat{h}_2^{(N)}(t,t)$, $\hat{h}_3^{(N)}(t,t,t),\ldots,$ $\hat{h}_N^{(N)}(t,\ldots,t)$ [26], [28].

Responses of the investigated EMS models are generally calculated based on expressions:

$$\tilde{y}_j(t\,|\,a_j) = a_j\hat{y}_1(t) + a_j^2\hat{y}_2(t) + \ldots + a_j^N\hat{y}_N(t),\quad j=\overline{1,L}, \quad (8)$$

or

$$\tilde{y}(t\,|\,a_j) = a_j\hat{h}_1^{(N)}(t) + a_j^2\hat{h}_2^{(N)}(t,t) + \\ + \ldots + a_j^N\hat{h}_N^{(N)}(t,\ldots,t),\quad j=\overline{1,L} \quad . \quad (9)$$

Fig. 2 presents the structural scheme, as described in [26], for calculating the transient characteristics based on the LSM. The scheme represents a second-order model, where block T_2 computes the first- and second-order transient characteristics based on the system of normal equations (7). The matrix A_2 in block T_2 incorporates all three input step signals (a_1, a_2, a_3) in the form of Heaviside function.

The operation of block T_2 and the matrix A_2 are described by the following formulas:

$$T_2 = \left(A_2' A_2\right)^{-1} A_2';\ A_2 = \begin{bmatrix} a_1 & a_1^2 \\ a_2 & a_2^2 \\ a_3 & a_3^2 \end{bmatrix}.$$

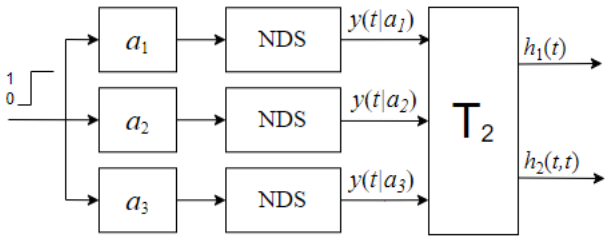

Fig. 2. **Structural scheme for computing the first- and second-order transient characteristics using the LSM identification method**
Source: **compiled by the authors**

Compensation Identification Method. The formalism of the method for determining the intersections of *n*-th order transient characteristics of nonlinear dynamic systems is based on the following assertion [26], [28].

Assertion 3. Let the test inputs be the sum of *n* step signals $x_k(t) = a_k\theta(t-\tau_k)$ (k=1, 2,...,n), shifted in time by τ_1, ..., τ_n. Then, for an NDS with a single input and a single output, the estimate of the intersection of the *n*-th order transient characteristic is

$$\hat{h}_n(t-\tau_1,\ldots,t-\tau_n) = \\ = \left(n!\prod_{k=1}^{n}a_k\right)^{-1}\sum_{\delta_1,\ldots,\delta_n=0}^{1}(-1)^{n+\sum_{k=1}^{n}\delta_k}\,y(t\,|\,\delta_1,\ldots,\delta_n) \quad (10)$$

where $y(t\,|\,\delta_1,\ldots,\delta_n)$ is the NDS response at time t when subjected to a multi-step input signal with amplitudes a_k, obtained as a result of processing experimental data based on (10). If $\delta_k = 1$, the test input contains a step signal shifted by τ_k; otherwise, if $\delta_k = 0$, it does not contain it.

In certain cases, we have:
for n=1

$$\hat{h}_1(t) = \frac{y(t\,|a_1)}{a_1} + \Delta_1; \quad (11)$$

for n=2

$$\hat{h}_2(t,t) = \frac{1}{2a_1^2}\left[y(t\,|a_2) - 2y(t\,|\,a_1)\right] + \Delta_2; \quad (12)$$

or

$$\hat{h}_2(t,t) = \frac{1}{2a_1a_2}\left[y(t\,|a_3) - y(t\,|\,a_1) - y(t\,|a_2)\right] + \Delta_2; \quad (13)$$

for n=3

$$\hat{h}_3(t,t,t) = \frac{1}{6a_1^3}\left[y(t\,|a_3) - 3y(t\,|\,a_2) + 3y(t\,|\,a_1)\right] + \Delta_3. \quad (14)$$

where a_1, $a_2 = 2a_1$, $a_3 = a_1 + a_2$ are the amplitudes of test signals; Δ_n represents the methodological error resulting from the discarded terms of the IPS of order n+1 and higher.

The responses of the second and third-order models are calculated accordingly using the expressions:

$$\tilde{y}(t\,|\,a_j) = a_j\hat{h}_1(t) + a_j^2\hat{h}_2(t,t)\ , \quad (15)$$

$$\tilde{y}(t\,|\,a_j) = a_j\hat{h}_1(t) + a_j^2\hat{h}_2(t,t) + a_j^3\hat{h}_3(t,t,t)\ ,\ \forall j=\overrightarrow{1,L}\ . \quad (16)$$

The compensation identification method is presented with a structural scheme illustrating the calculations based on formula (12), as shown in Fig. 3. This scheme demonstrates the process of obtaining of the diagonal cross-section of the second-order transient characteristics using two test signals with amplitudes a_1 and a_2 in the form of the Heaviside function. In Fig. 4, the same scheme is shown for the transient characteristic obtained using three test signals in the form of the Heaviside function, with amplitudes a_1, a_2 and a_3, as described in formula (13).

ISSN 2617-4316 (Print)
ISSN 2663-7723 (Online)

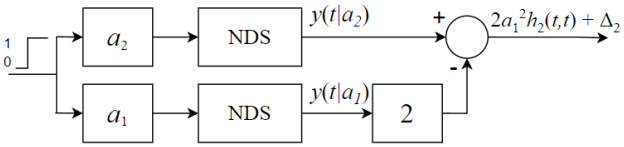

Fig. 3. **Structural scheme for computing the diagonal cross-section of the second-order transient characteristic using the compensation method with two test signals**
Source: **compiled by the authors**

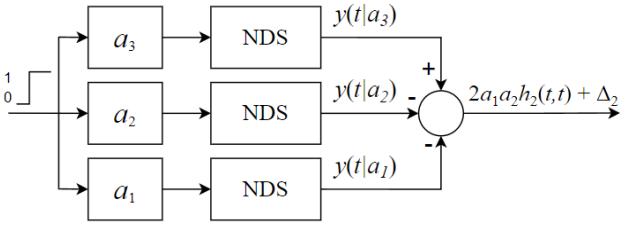

Fig. 4. **Structural scheme for computing the diagonal cross-section of the second-order transient characteristic using the compensation method with three test signals**
Source: **compiled by the authors**

4. ACCURACY ANALYSIS OF EYE MOVEMENT SYSTEM SIMULATION MODELS

The EMS's responses to the test step signals, defined as $x(t)=a_j\Theta(t)$ with amplitudes a_j (j=1, 2, 3): a_1=1/3, a_2=2/3, a_3=1 were analyzed. These responses formed the basis in the construction of Volterra models [24]. Horizontal visual stimuli displayed at varying distances from the starting position on a monitor were utilized as test signals, effectively simulating the application of step signals with different amplitudes to the EMS. The responses of the EMS were recorded using eye-tracking technology, integrating both hardware and software components. In the simulation process, when applying the approximation method, models based on IPS are identified as M1.N/x:<a_1,…, a_L> (N – order of approximation, x – number of test signals; a_1,…, a_L – amplitudes of the test step signals). For models based on IPP, the least squares method (LSM) is used, resulting in models designated as M2.N/x:<a_1,…, a_L>. Additionally, when employing the compensation method of simulation, models are determined as M3.N/x:<a_1,…, a_L>.

For EMS simulation in works [28]–[31], experimental "input-output" data were gathered using three test step signals with amplitudes a_1=1/3, a_2=2/3 and a_3=1. The Tobii Pro TX300 eye tracker was employed to collect these experimental data (Fig. 5), from which transient characteristics were determined for models M1.N, M2.N, and M3.N for N=1 (linear model), N=2 (quadratic model), and N=3 (cubic model). The transient processes of EMS responses to visual stimuli with varying amplitudes are depicted in Fig. 6.

The software tools were developed using the Python programming environment.

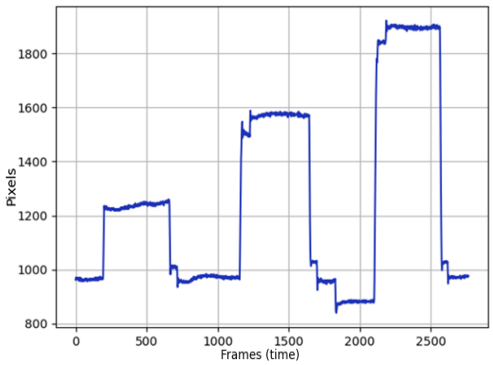

Fig. 5. **EMS responses to visual stimuli of different amplitudes**
Source: **compiled by the authors**

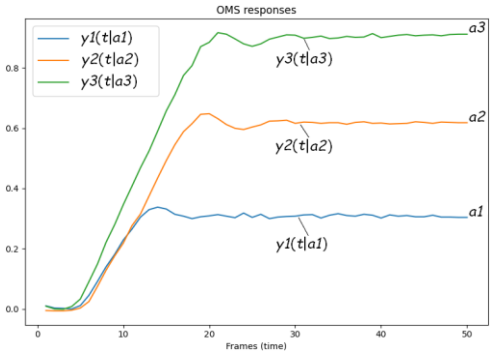

Fig. 6. **Transient processes of EMS responses to visual stimuli of different amplitudes**
Source: **compiled by the authors**

To evaluate the accuracy of the developed models for varying amplitudes of the test signals a_1, a_2 and a_3, the metric applied is the normalized root mean square error (NRMSE):

$$\varepsilon_{a_j}=\left(\frac{\sum_{m=0}^{M}\left(y(t_m\,|\,a_j)-\tilde{y}(t_m\,|\,a_j)\right)^2}{\sum_{m=0}^{M}y^2(t_m\,|\,a_j)}\right)^{1/2},\quad j=1,\,2,\,3; \qquad (17)$$

where $y(t_m\,|\,a_j)$ and $\tilde{y}(t_m\,|\,a_j)$ are the responses of the EMS and the model of the EMS to the test signal in the form of a step function with amplitude a_j, measured/ computed at the time instant t_m (t_m is the observation time of the EMS responses); j=1,2,3.

For N=1, transient characteristics $\hat{h}_1(t\,|\,a_j)$ (j=1, 2, 3) were obtained based on the responses $y(t\,|\,a_1)$ or $y(t\,|\,a_2)$ or $y(t\,|\,a_3)$, as shown in Fig. 7.

Fig. 8 shows transient characteristics graphs of the M2.1/2 models, which were calculated based on two responses: $y(t|a_1)$ and $y(t|a_2)$, or $y(t|a_1)$ and $y(t|a_3)$, or $y(t|a_2)$ and $y(t|a_3)$ and the transient characteristic graph of the model M2.1/3. For the M1.1 identification method does not allow to calculate the transient characteristics based on two or three responses [26].

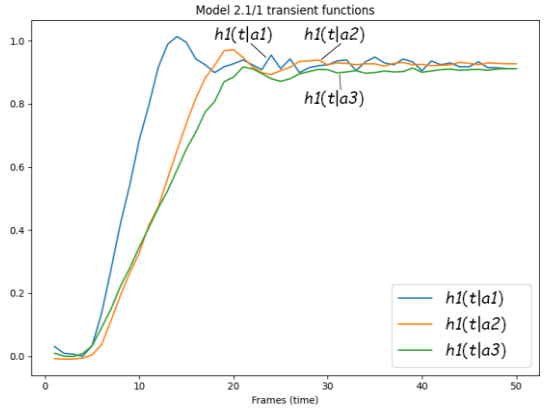

Fig. 7. **Transient characteristics of the EMS models M1.1/1 and M2.1/1, built using test signals with amplitudes a_1; a_2; a_3**
Source: **compiled by the authors**

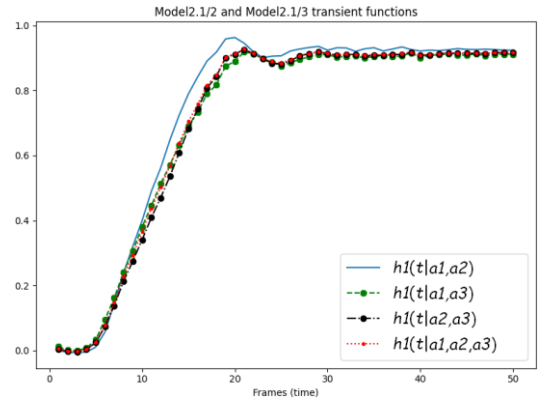

Fig. 8. **Transient characteristics of the EMS models M2.1/2, built using test signals with amplitudes: a_1 and a_2; a_1 and a_3; a_2 and a_3; and M2.1/3**
Source: **compiled by the authors**

For the compensation identification method, the model M3.1 based on the response $y(t|a_1)$ was derived. The corresponding transient characteristic is illustrated in Fig. 9, while the model's responses are depicted in Fig. 10.

Table 1 shows the accuracy values based on percentage NRMSE estimates of the responses obtained using the identification methods for EMS models M1.1/1, M2.1/1, and M3.1, while Table 2 presents the values for models M2.1/2 and M2.1/3.

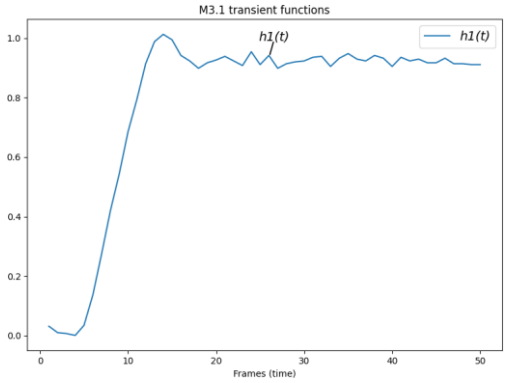

Fig. 9: **Transient characteristic of the EMS model M3.1 built using test signal with amplitude a_1**
Source: **compiled by the authors**

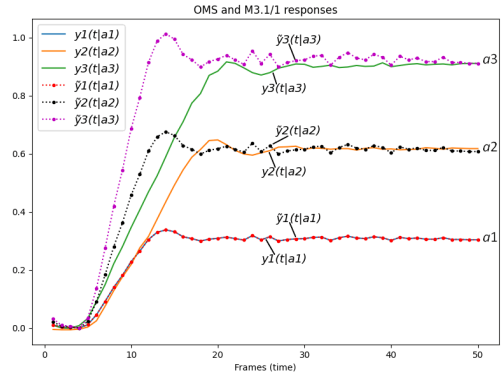

Fig. 10. **Responses of the EMS and the model M3.1 built using test signal with amplitude a_1**
Source: **compiled by the authors**

Table 1. **Accuracy based on Percentage Normalized Root Mean Square Error of the EMS models M1.1/1, M2.1/1 and M3.1 %**

Models	Amplitudes of test signals			Mean value
	a_1	a_2	a_3	
M1.1/1:a_1	99.9	81.8	79.7	80.8
M1.1/1:a_2	82.8	99.9	94.5	88.6
M1.1/1:a_3	81.5	94.7	99.9	88.1
M3.1:a_1	99.9	82	80	81

Source: **compiled by the authors**

Table 2. **Accuracy Based on Percentage Normalized Root Mean Square Error of the EMS models M2.1/2 and M2.1/3 %**

Models	Amplitudes of test signals			Mean value
	a_1	a_2	a_3	
M2.1/2:a_1,a_2	86.2	96.4	92.9	91.8
M2.1/2:a_1,a_3	83.3	95.1	98.0	92.1
M2.1/2:a_2,a_3	82.0	96.3	98.3	92.2
M2.1/3:a_1,a_2,a_3	83.3	96.5	97.5	92.4

Source: **compiled by the authors**

ISSN 2617-4316 (Print)
ISSN 2663-7723 (Online)

For N=2, based on the two responses $y(t \mid a_1)$ and $y(t \mid a_2)$, or $y(t \mid a_1)$ and $y(t \mid a_3)$, or $y(t \mid a_2)$ and $y(t \mid a_3)$, the corresponding multidimensional transient characteristics $\hat{h}_1(t|a_j,a_k)$ and $\hat{h}_2(t,t|a_j,a_k)$, $j, k = 1,2,3; j \neq k$ were obtained. In the models M1.2/2 and M2.2/2, identical MTCs $\hat{h}_1(t|\ a_j,a_k)$ and $\hat{h}_2(t\ ,t|\ a_j,a_k)$ were obtained for the same experimental data.

Fig. 11 displays both the first-order transient characteristics and the diagonal cross-sections of the second-order MTCs for the EMS models M1.2/2 and M2.2/2. Both the first- and second-order transient characteristics were computed based on the responses: $y(t \mid a_1)$ and $y(t \mid a_2)$, or $y(t \mid a_1)$ and $y(t \mid a_3)$, or $y(t \mid a_2)$ and $y(t \mid a_3)$.

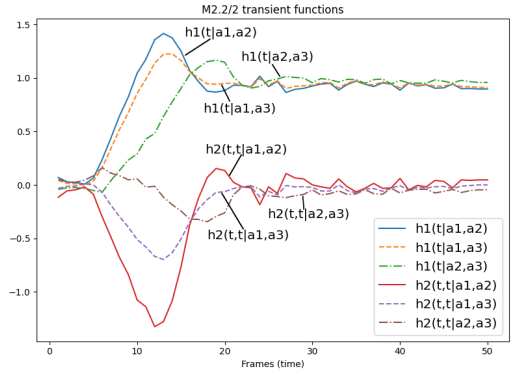

Fig. 11. **Transient characteristics of the first-order and diagonal cross-sections of the second-order of the EMS, models M1.2/2 and M2.2/2**
Source: **compiled by the authors**

The transient characteristics of the EMS model M3.2/2 are illustrated in Fig. 12. The corresponding responses for the same model are given in Fig. 13.

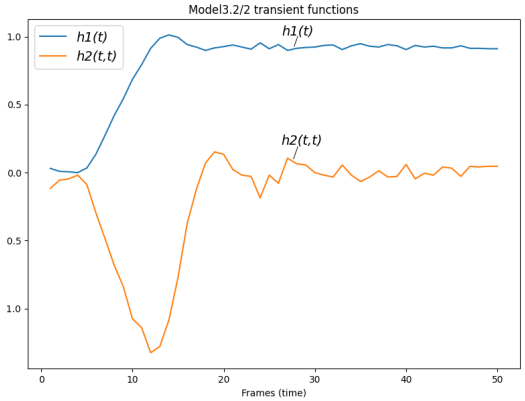

Fig. 12. **Multidimensional transient characteristics of the EMS, model M3.2/2**
Source: **compiled by the authors**

The graphs of the multidimensional transient characteristics $\hat{h}_1(t)$ and $\hat{h}_2(t,t)$, which were determined based on the three responses $y(t \mid a_1)$, $y(t \mid a_2)$, $y(t \mid a_3)$ for the EMS model M2.2/3, are shown in Fig. 14.

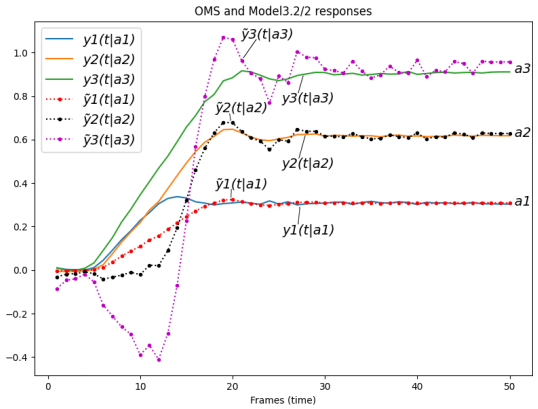

Fig. 13. **Responses of the EMS and the model M3.2/2**
Source: **compiled by the authors**

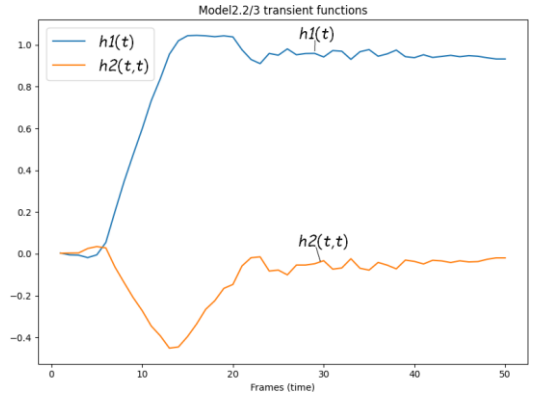

Fig. 14. **Multidimensional transient characteristics of the EMS, model M2.2/3**
Source**: compiled by the authors**

The corresponding graphs comparing the M2.2/3 responses with the EMS responses to identical test signals are presented in Fig. 15. Analogous results were obtained for the M3.2/3 and are shown in Fig. 16 and Fig. 17.

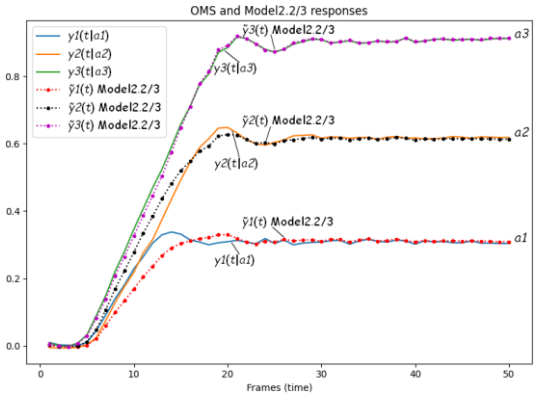

Fig. 15. **Responses of the EMS and the model M2.2/3**
Source: **compiled by the authors**

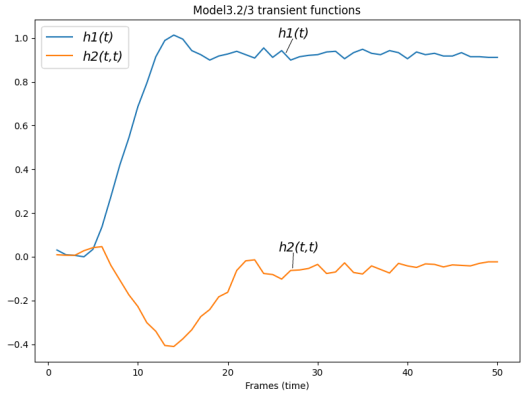

Fig. 16. **Multidimensional transient characteristics of the EMS, model M3.2/3**
Source: **compiled by the authors**

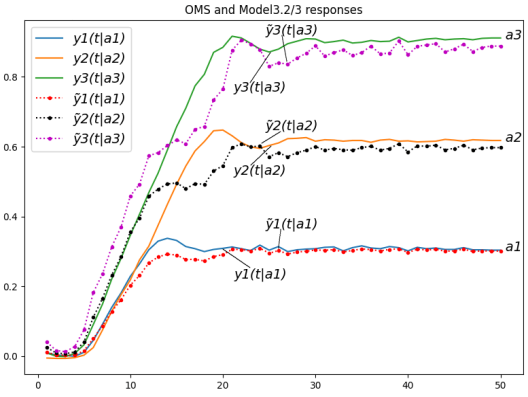

Fig. 17. **Responses of the EMS and the model M3.2/3**
Source: **compiled by the authors**

For N=3, the graph of the primary-order transient characteristic, along with the graphs of the diagonal cross-sections of the second and third-order multidimensional transient characteristics for the EMS model M3.3, are displayed in Fig.18. The responses of the EMS model M3.3 are shown in Fig.19.

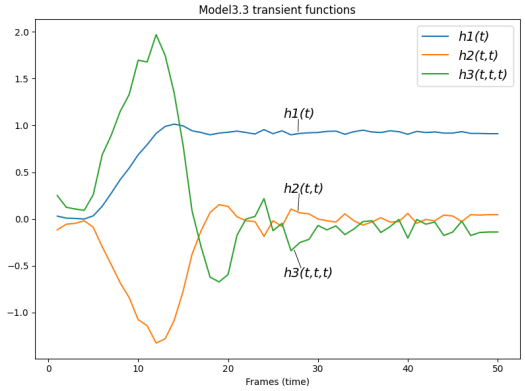

Fig. 18. **Multidimensional transient characteristics of the EMS model M3.3**
Source: **compiled by the authors**

Table 3 provides the accuracy values based on percentage normalized root mean square error of the response estimates for the constructed EMS models M1.2/2 and M2.2/2, and the model M2.2/3. Table 4 presents the accuracy values for the models M3.2/2 and M3.2/3, and the model M3.3/3.

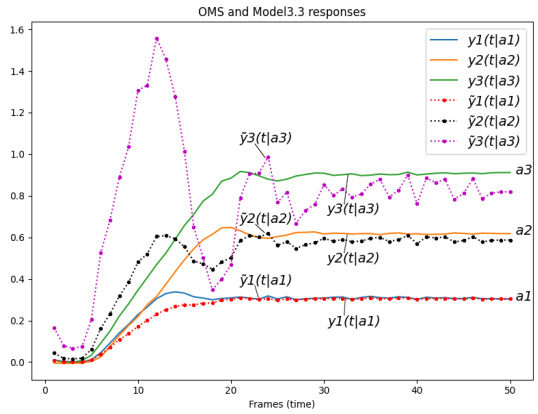

Fig. 19. **Responses of the EMS and the model M3.3**
Source: **compiled by the authors**

Table 3. **Accuracy Based on Percentage Normalized Root Mean Square Error of the EMS models M1.2/2, M2.2/2 and M2.2/3, %**

Model	Amplitudes of test signals			Mean value
	a_1	a_2	a_3	
M2.2/2:a_1,a_2	99.9	99.9	81.0	81.0
M2.2/2:a_1,a_3	99.9	90.9	99.9	90.9
M2.2/2:a_2,a_3	82.7	99.9	99.9	82.7
M2.2/3:a_1,a_2,a_3	91.8	95.7	99.0	95.5

Source: **compiled by the authors**

Table 4. **Accuracy Based on Percentage Normalized Root Mean Square Error of the EMS models M3.2/2, M3.2/3 and M3.3, %**

Model	Amplitudes of test signals			Mean value
	a_1	a_2	a_3	
M3.2/2:a_1,a_2	82.8	81.8	62.6	75.7
M3.2/3:a_1,a_2,a_3	93.9	88.7	92.2	91.6
M3.3/3:a_1,a_2,a_3	90.7	80.1	51.4	74.1

Source: **compiled by the authors**

For N=3, based on the three responses $y(t \mid a_1)$, $y(t \mid a_2)$, $y(t \mid a_3)$ the transient characteristics $\hat{h}_1(t)$, $\hat{h}_2(t,t)$, $\hat{h}_3(t,t,t)$ were obtained. For the models M1.3/3 and M2.3/3, identical MTCs were obtained, and the responses of the models practically coincide with the responses of the EMS for the same input signals.

On Fig. 20, a comparative analysis diagram of the accuracy based on the percentage NRMSE criterion constructed using identification software tools for EMS models: M2.1/1, M2.1/2, M2.1/3, is presented.

On Fig. 21, the same analysis is provided for models M2.2/2, M3.2/2, M2.2/3, M3.2/3 and M3.3.

ISSN 2617-4316 (Print)
ISSN 2663-7723 (Online)

The EMS model M2.3 are not shown in the diagram because it have negligible deviations from the EMS responses.

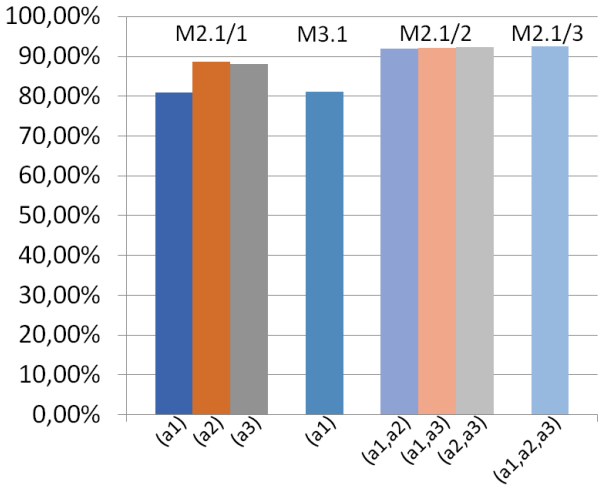

Fig. 20. **Comparative analysis of the accuracy based on the average percentage NRMSE values of the EMS models: M2.1/1; M3.1; M2.1/2; M2.1/3**

Source: **compiled by the authors**

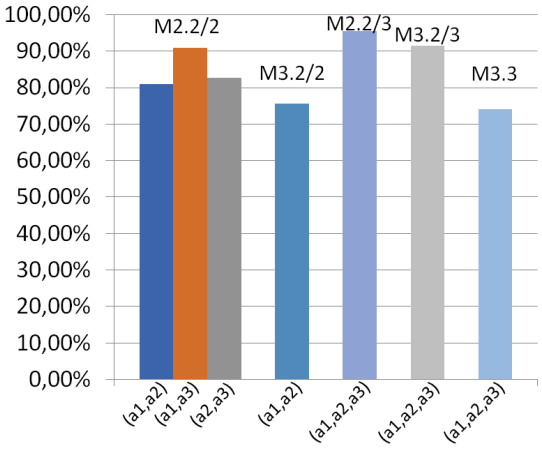

Fig. 21. **Comparative analysis of the accuracy based on the average percentage NRMSE values of the EMS models: M2.2/2; M3.2/2; M2.2/3; M3.2/3; M3.3**

Source: **compiled by the authors**

5. CONCLUSION

This study applied Python-implemented nonlinear dynamic simulation of the human EMS, utilizing integro-power series and integro-power polynomials to develop models that accurately reflect the eye movement system's response dynamics. By employing the least squares method, compensation, and approximation methods, we evaluated various model accuracies based on first-order transient characteristics and diagonal cross-sections of second- and third-order multidimensional transient characteristics. The data for these models was collected from eye-tracking experiments designed to capture responses to test signals with varying amplitudes.

The results demonstrate that the quadratic model, developed using three test signal responses and refined with the least squares method, provided the highest simulation accuracy and computational efficiency, outperforming alternative models in precision. The evaluation showed a significant reduction in error rates as more test signals were incorporated, highlighting the value of using multiple data points for improved accuracy. While the compensation method required fewer computational resources, it exhibited higher error rates, making it less suitable for applications requiring high diagnostic precision. It is important to note that the models of the third order and the second-order model based on the compensation method using two test signals yield unstable solutions.

In summary, the quadratic model using the least squares method and three test signals provides a reliable framework for EMS-based state classification. The developed models, particularly the quadratic IPP model, offer a robust foundation for further research into personalized psychophysiological condition assessment through the development of classifiers. This methodology enables high accuracy in EMS simulation and effective psychophysiological condition assessment, providing a strong basis for future studies and EMS-related applications.

REFERENCES

1. Opwonya, J., Doan, D. N. T., Kim, S. G., et al. "Saccadic Eye movement in mild cognitive impairment and alzheimer's disease: A systematic review and meta-analysis". *Neuropsychol Rev.* 2022; 32: 193–227. DOI: https://doi.org/10.1007/s11065-021-09495-3.

2. Sun, J., Liu, Y., Wu, H., Jing, P. & Ji, Y. "A novel deep learning approach for diagnosing Alzheimer's disease based on eye-tracking data". *Front. Hum. Neurosci.* 2022; 16: 972773. DOI: https://doi.org/10.3389/fnhum.2022.972773.

3. Tokushige, S. I., Matsumoto, H., Matsuda, S. I., et al. “Early detection of cognitive decline in alzheimer’s disease using eye tracking”. *Front. Aging Neurosci.* 2023; 15: 1123456. DOI: https://doi.org/10.3389/fnagi.2023.1123456.

4. Ștefănescu, E., Chelaru, V. F., Chira, D. & Mureșanu, D. “Eye tracking assessment of parkinson's disease: a clinical retrospective analysis”. *J. Med. Life.* 2024; 17 (3): 360. DOI: https://doi.org/10.25122/jml-2024-0270.

5. Veerapa, E., Grandgenevre, P., Vaiva, G., et al. “Attentional bias toward negative stimuli in PTSD: an eye-tracking study”. *Psychological Medicine.* 2023; 53 (12): 5809–5817. DOI: https://doi.org/10.1017/S0033291722003063.

6. Keehn, B., Monahan, P., Enneking, B., et al. “Eye-tracking biomarkers and autism diagnosis in primary care”. *JAMA Netw Open.* 2024; 7 (5): e2411190. DOI: https://doi.org/10.1001/jamanetworkopen. 2024.11190.

7. Dostálová, N., Pátková Daňsová, P., Ježek, S., Vojtechovska, M. & Šašinka, Č. “Towards the Intervention of Dyslexia: a Complex Concept of Dyslexia Intervention System using Eye-Tracking”. *In Proceedings of the 2024 Symposium on Eye Tracking Research and Applications (ETRA '24).* 2024. Article 84. DOI: https://doi.org/10.1145/3649902.3656490.

8. Kasprowski, P. “Utilizing gaze self similarity plots to recognize dyslexia when reading”. *In Proceedings of the 2024 Symposium on Eye Tracking Research and Applications (ETRA).* 2024. Article 85. DOI: https://doi.org/10.1145/3649902.3656494.

9. Chandran, P., Huang, Y., Munsell, J., et al. “Characterizing learners' complex attentional states during online multimedia learning using eye-tracking, Egocentric Camera, Webcam, and Retrospective recalls”. *In Proceedings of the 2024 Symposium on Eye Tracking Research and Applications (ETRA).* 2024. DOI: https://doi.org/10.1145/3649902.3653939.

10. Sun, W., Wang, Y., Hu, B. & Wang, Q. “Exploring the connection between eye movement parameters and eye fatigue”. *J. Phys.: Conf. Ser.* 2024; 2722: 012013. DOI: https://doi.org/10.1088/1742-6596/2722/1/012013.

11. Sun, W., Wang, Y., Hu, B. & Wang, Q. “Exploration of eye fatigue detection features and algorithm based on eye-tracking signal”. *Electronics.* 2024; 13 (10): 1798. DOI: https://doi.org/10.3390/electronics13101798.

12. Weiss, K., Kolbe, M., Lohmeyer, Q. & Meboldt, M. “Measuring teamwork for training in healthcare using eye tracking and pose estimation”. *Front. Psychol.* 2023; 4: 1169940. DOI: https://doi.org/10.3389/fpsyg.2023.1169940.

13. Griffith, H., Lohr, D., Abdulin, E. & Komogortsev, O. “GazeBase, a large-scale, multi-stimulus, longitudinal eye movement dataset”. *Sci. Data, Nature.* 2021; 8: 13. DOI: https://doi.org/10.1038/s41597-021-00959-y.

14. Yin, J., Sun, J., Li, J., & Liu, K. “An effective gaze-based authentication method with the spatiotemporal feature of eye movement”. *Sensors.* 2022; 22: 3002. DOI: https://doi.org/10.3390/s22083002.

15. Jansson, D., Rosén, O., & Medvedev, A. “Parametric and nonparametric analysis of eye-tracking data by anomaly detection”. *IEEE Trans. Control Syst. Technol.* 2015; 23: 1578–1586. DOI: https://doi.org/10.1109/TSCT.2014.2364958.

16. Bro, V., & Medvedev, A. “Continuous and discrete Volterra-Laguerre models with delay for modeling of smooth pursuit eye movements”. *IEEE Trans. Biomed. Eng.* 2023; 70 (1): 97–104.

17. Lanata, L., Sebastian, L., Di Gruttola, F., et al. “Nonlinear analysis of eye-tracking information for motor imagery assessments”. *Front. Neurosci.* 2020; 13: 1431. DOI: https://doi.org/10.3389/ fnins.2019.01431.

18. Porras, M. M., Campen, C. A. N. Kv., González-Rosa, J. J., et al. “Eye tracking study in children to assess mental calculation and eye movements”. *Sci Rep.* 2024; 14: 18901. DOI: https://doi.org/10.1038/s41598-024-69800-x.

19. Hao, S., Jiaxin, J., Siping, F., et al. “Evaluating the Impact of mental workload on drillers' risk perception using wearable eye-tracking technology”. *SSRN.* 2024; 4925093. DOI: https://doi.org/10.2139/ssrn.4925093.

20. Kalla, B. V., Mandava, N. & Surya, C. “Eye disease detection using deep learning models with transfer learning techniques”. *ICST Trans. on Scalable Inf. Syst.* 2024; 11. DOI: https://doi.org/10.4108/eetsis.5971.

21. Jyotsna, C., Amudha, J., Ram, A., Fruet, D. & Nollo, G. “PredictEYE: Personalized time series model for mental state prediction using eye tracking”. *IEEE Access*. 2023; 11: 128383–128409. DOI: https://doi.org/10.1109/ACCESS.2023.3332762.

22. Solodusha, S., Kokonova, Y. & Dudareva, O. “Integral models in the form of Volterra polynomials and continued fractions in the problem of identifying input signals”. *Mathematics*. 2023; 11 (23): 4724. DOI: https://doi.org/10.3390/math11234724.

23. Doyle, F. J., Pearson, R. K. & Ogunnaike, B. A. “Identification and control using Volterra models”. *Springer, London*. 2001.

24. Pavlenko, V., Milosz, M. & Dzienkowski, M.., “Identification of the Oculo-Motor system based on the Volterra model using eye tracking technology”. *Journal of Physics: Conference Series*. 2020; 1603: 1–8. DOI: https://doi.org/10.1088/1742-6596/1603/1/012011.

25. Pavlenko, V. D., Salata, D. V. & Chaikovskyi, H. P. “Identification of an Oculo-Motor system human based on Volterra kernels”. *Int. J. Biol. Biomed. Eng.* 2017; 11: 121–126.

26.Pavlenko, V. & Pavlenko, S. “Deterministic identification methods for nonlinear dynamical systems based on the Volterra model”. *Applied Aspects of Information Technology*. 2018; 1 (1): 9–29. DOI: https://doi.org/10.15276/aait.01.2018.1.

27. Pavlenko, V., Pavlenko, S. & Speranskyy, V. “Identification of systems using Volterra model in time and frequency domain”. *Advanced Data Acquisition and Intelligent Data Processing. River Publishers*. 2014. p. 233–270.

28. Pavlenko, V., Shamanina, T. & Chori, V. “Biometric identification based on the multidimensional transient functions of the human oculo-motor system”. *Journal of Physics: Conference Series*. 2022; 2162: 012024. DOI: https://doi.org/10.1088/1742-6596/2162/1/012024.

29. Pavlenko, V., Shamanina, T. & Chori, V. “Nonlinear dynamics identification of the oculo-motor system based on eye tracking data”. *International Journal of Circuits, Systems and Signal Processing*. 2021; 15: 569–577. DOI: https://doi.org/10.46300/9106.2021.15.63.

30. Pavlenko, V. & Shamanina, T. “Eye-tracking technology in smart system for monitoring of human’s psychophysiological states”. *Lecture Notes in Networks and Systems*. 2023; 629: 344–353.

31.Pavlenko, V. D., Shamanina, T. V. & Chori, V. V. “Application of nonlinear dynamic models of the oculo-motor system in diagnostic studies in neurosciences”. *Journal of Neuroscience and Neurological Disorders*. 2023; 07 (02): 126–133. DOI: https://www.neuroscijournal.com/articles/jnnd-aid1086.pdf.

Conflicts of Interest: The authors declare that they have no conflict of interest regarding this study, including financial, personal, authorship or other, which could influence the research and its results presented in this article

Received 30.08.2024
Received after revision 25.10.2024
Accepted 11.11.2924

DOI: https://doi.org/10.15276/aait.07.2024.20
УДК 681.5.015.52

Оцінки точності ідентифікації око-рухової системи людини за допомогою ступінчатих тестових сигналів

Павленко Віталій Данилович[1)]
ORCID: https://orcid.org/0000-0002-5655-4171; pavlenko_vitalij@ukr.net. Scopus Author ID: 54401442600
Лукашук Денис Костянтинович[1)]
ORCID: https://orcid.org/0009-0003-3149-3741; user111228322@gmail.com
[1)] Національний університет «Одеська політехніка», пр. Шевченко,1.Одеса, 65044, Україна

АНОТАЦІЯ

У цьому дослідженні вивчаються методи ідентифікації нелінійних динамічних систем для моделювання око-рухової системи (ОРС) людини, з акцентом на точне представлення перехідних характеристик, отриманих із ступінчатих тестових сигналів. Інтегральні нелінійні моделі були застосовані для врахування нелінійної динаміки та інерційних властивостей ОРС. Експериментальні дані «вхід-вихід» були зібрані за допомогою сучасної технології айтрекінгу, що дозволило ідентифікувати багатовимірні перехідні характеристики (БПХ), які описують динамічну поведінку ОРС у відповідь на

візуальні стимули. У дослідженні було використано методи апроксимації та компенсації для розробки моделей на основі інтегро-степеневих рядів (ІСР), а також метод найменших квадратів (МНК) для побудови моделей на основі інтегро-степеневих поліномів (ІСП). Метод компенсації, хоч і є менш обчислювально вимогливим, продемонстрував нижчу точність, що обмежує його застосування для завдань, які потребують високої точності. Моделі третього порядку виявили нестабільність у своїх перехідних характеристиках, що обмежує їх практичне використання. Моделі другого порядку, зокрема квадратичні моделі ІСП, розроблені за допомогою МНК, виявилися найточнішими та найефективнішими з точки зору обчислень. Ці моделі забезпечили точне й узгоджене представлення динаміки ОРС, із значним зменшенням рівня похибок при використанні трьох тестових сигналів замість двох. Це підкреслює важливість достатньої кількості даних для підвищення надійності моделей. Результати підтверджують придатність квадратичної моделі ІСП, уточненої методом найменших квадратів, для подальших досліджень. Ця модель забезпечує надійну основу для розвитку досліджень у сфері персоналізованої оцінки психофізіологічних станів шляхом створення класифікаторів. Її точність і стабільність роблять її цінним інструментом для вивчення методів класифікації станів у медичній сфері, когнітивних науках та інших галузях, що вимагають точного моделювання динамічних систем.

Ключові слова: око-рухова система; моделювання; моделі Вольтерри; технологія айтрекінгу; точність моделювання; нейрофізіологічний стан

ABOUT THE AUTHORS

Vitaliy D. Pavlenko - Doctor of Engineering Sciences, Professor, Department “Computerized Systems and Software Technologies”. Odesa Polytechnic National University, Shevchenko Ave. 1, Odesa, 65044, Ukraine
ORCID: https://orcid.org/0000-0002-5655-4171; pavlenko_vitalij@ukr.net. Scopus Author ID: 54401442600
***Research field*:** Math modeling and simulation; Volterra models; nonlinear dynamic identification; intelligent information technologies; machine learning; technical and medical diagnostics; neuroscience; biometric identification; innovation eye-tracking technology

Павленко Віталій Данилович - доктор технічних наук, професор, професор кафедри «Комп’ютеризовані системи та програмні технології» Національного університету «Одеська політехніка», пр. Шевченка, 1. Одеса, 65044, Україна

Denys K. Lukashuk - Postgraduate Student, Department “Computerized Systems and Software Technologies” Odesa Polytechnic National University, Shevchenko Ave. 1, Odesa, 65044, Ukraine
ORCID: https://orcid.org/0009-0003-3149-3741; user111228322@gmail.com
***Research field*:** Software engineering; mathematical modeling; machine learning; neural network technologies; eye-tracking technology.

Лукашук Денис Костянтинович - аспірант кафедри «Комп’ютеризовані системи та програмні технології» Національного університету «Одеська політехніка», пр. Шевченка, 1. Одеса, 65044, Україна